ORGANOMETALLICS

pubs.acs.org/Organometallics

Article

Bromination and C−C Cross-Coupling Reactions for the C−H Functionalization of Iridium(III) Emitters

Pierre-Luc T. Boudreault, Miguel A. Esteruelas,* Erik Mora, Enrique Oñate, and Jui-Yi Tsai

Cite This: *Organometallics* 2021, 40, 3211−3222

Read Online

ACCESS | Metrics & More | Article Recommendations | Supporting Information

ABSTRACT: The orthometalated phenyl groups of the dimer $[Ir(\mu\text{-Cl})\{\kappa^2\text{-}C,N\text{-}(C_6H_3Me\text{-}py)\}_2]_2$ have been selectively brominated, at *para*-position with regard to the Ir−C bonds, with *N*-bromosuccinimide. The bromination leads to $[Ir(\mu\text{-Cl})\{\kappa^2\text{-}C,N\text{-}(C_6H_2MeBr\text{-}py)\}_2]_2$, which affords the mononuclear derivatives $Ir\{\kappa^2\text{-}C,N\text{-}(C_6H_2MeBr\text{-}py)\}_2\{\kappa^2\text{-}O,N\text{-}[OC(O)\text{-}py]\}$, $Ir\{\kappa^2\text{-}C,N\text{-}(C_6H_2MeBr\text{-}py)\}_2\{\kappa^2\text{-}O,O\text{-}(acac)\}$, and $Ir\{\kappa^2\text{-}C,N\text{-}(C_6H_2MeBr\text{-}py)\}_2\{\kappa^2\text{-}C,N\text{-}[C_6H_4\text{-}Mepy]\}$ by replacement of the chloride bridges by a picolinate anion, an acac group, and an orthometalated 2-phenyl-5-methylpyridine ligand, respectively. Complexes $Ir\{\kappa^2\text{-}C,N\text{-}(C_6H_2MeBr\text{-}py)\}_2\{\kappa^2\text{-}O,O\text{-}(acac)\}$ and $Ir\{\kappa^2\text{-}C,N\text{-}(C_6H_2MeBr\text{-}py)\}_2\{\kappa^2\text{-}C,N\text{-}[C_6H_4\text{-}Mepy]\}$ have been subsequently post-functionalized by means of palladium-catalyzed Suzuki−Miyaura cross-coupling to give $Ir\{\kappa^2\text{-}C,N\text{-}(C_6H_2MeR\text{-}py)\}_2\{\kappa^2\text{-}O,O\text{-}(acac)\}$ (R = Me, Ph) and $Ir\{\kappa^2\text{-}C,N\text{-}(C_6H_2Me_2\text{-}py)\}_2\{\kappa^2\text{-}C,N\text{-}[C_6H_4\text{-}Mepy]\}$. These [3b + 3b + 3b′] mononuclear compounds are green-yellow emitters (488−580 nm) upon photoexcitation, in doped poly(methyl methacrylate) (PMMA) film at 5 wt % at room temperature and 2-methyltetrahydrofuran (2-MeTHF) at room temperature and at 77 K. They display lifetimes in the range 1.0−5.0 μs and quantum yields in PMMA films and in 2-MeTHF at room temperature between 0.84 and 0.40.

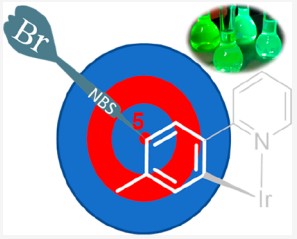

INTRODUCTION

The selective functionalization of inactivated C−H bonds is a target of paramount importance for modern chemistry. Particularly relevant is the functionalization of aromatic compounds because of the wide range of applications of these moieties in several fields, including material science. Traditional electrophilic aromatic substitution reactions are directed by the substituents of the arene. Electron donating groups promote substitutions at *ortho*- and *para*-positions, whereas electron-withdrawing groups direct the electrophile to *meta*-position, although rather harsh conditions are necessary for the reaction. In the past years, metal-catalyzed C−H bond functionalization has emerged as a promising alternative. However, only the functionalization at *ortho*-position appears to be well solved, while the C−H functionalization of the *meta*- and *para*-positions continues to be extremely challenging.[1]

Halides are versatile functional groups in organic synthesis. In recent years, with the advent of cross-coupling chemistry, the importance of aryl-halides has been increased further, being currently classified as core building blocks in chemical synthesis.[2] Traditional routes to form a carbon−halogen bond generally afford poor regio- and chemoselectivities and need harsh reaction conditions, which are compatible with a scarce number of functional groups. To overcome these issues, interesting metal-catalyzed direct C−H halogenation reactions are being developed.[3] Particular interest is aroused by bromination, when the halide should be used as intermediate for cross-coupling chemistry, since the strength of the C−halide bonds decreases as we go down the group in the periodic table.[4]

Bromination can be carried out using molecular bromine.[5] However, it is hazardous and strongly irritant, and its reactions are rarely selective. As a result, different brominating reagents have been developed. Among them, *N*-bromosuccinimide (NBS) occupies a prominent place by its accessibility, easy handling, and reasonable stability.[4,6] With this reagent as bromine source, Ackermann and co-workers have disclosed a heterogeneous ruthenium catalyst for the *meta*-selective C−H bromination of arylpyridines and purines,[7] whereas Huang and co-workers have developed a homogeneous ruthenium-system for the *meta*-selective bromination of arenes bearing pyridyl, pyrimidyl, and pyrazolyl groups.[8] The mechanistic proposal includes the formation of a key intermediate coordinating two orthometalated aryl-substituted heterocycles. The metal center seems to direct the addition to its *para*-position of the resulting electron-rich arene. In agreement with this, Aoki and co-workers have described the selective bromination of the C−H bond disposed in *para* with regard to the C−M bond of orthometalated 2-aryl-pyridine chromophores, in homoleptic and heteroleptic phosphorescent iridium(III) emitters.[9] DFT calculations located a noticeable percentage of the HOMO of the precursor at the brominated position. Several groups[10] had

Received: July 9, 2021
Published: September 15, 2021

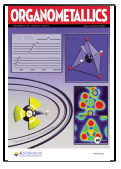

https://doi.org/10.1021/acs.organomet.1c00408
Organometallics 2021, 40, 3211−3222

previously employed pyridinium tribromide in the presence of a catalytic amount of iron powder or interhalogens in combination with a base (amines, carbonate, salts of carboxylic acids, etc.) and a Lewis acid, for the bromination of different class of σ-aryl organometallic compounds in *meta*-position with regard to the metal center, including also some homoleptic iridium(III) phosphorescent emitters[10c] and iridabenzene and iridabenzofuran complexes.[10d,e]

Molecular iridium(III) phosphorescent emitters lie at the forefront of modern photophysics[11] and photochemistry.[12] A class of emitters of noticeable interest is formed by compounds bearing three bidentate three-electron-donor ligands (3b), of two different types, usually two orthometalated 2-aryl-pyridines and other one. These molecules [3b + 3b + 3b′] are generally prepared from $[Ir(\mu\text{-Cl})(3b)_2]_2$ dimers.[13] Thus, the selective bromination of these starting materials should allow developing synthetic methodologies of postfunctionalization from the origin, reducing the issues of competitive functionalization and side reactions in subsequent steps. In the search for a proof of concept validation of this hypothesis, we decided to start from dimer $[Ir(\mu\text{-Cl})\{\kappa^2\text{-}C,N\text{-}(C_6H_3Me\text{-py})\}]_2$ (**1**) to develop a family of iridium(III) phosphorescent emitters, by means of the selective bromination of the phenyl groups at *para*-position with regard to the iridium atom, along with a subsequent cross-coupling chemistry.

This paper proves the performance of the methodology, reporting the preparation of three different types of brominated [3b + 3b + 3b′] emitters, their use as substrates for palladium-catalyzed cross-coupling reactions, and the photophysical properties of the resulting new emitters.

RESULTS AND DISCUSSION

Brominated Compounds. Treatment of dichloromethane solutions of complex **1** with 2 equiv of NBS, at room temperature, for 24 h produces the selective bromination of the phenyl substituent of the four orthometalated phenylpyridines, at *para*-position with regard to the iridium atom. Bromination of the metal center or Br/Cl exchange between the brominating reagent and complex **1** were not observed. The C−H functionalization reaction affords dimer $[Ir(\mu\text{-Cl})\{\kappa^2\text{-}C,N\text{-}(C_6H_2MeBr\text{-py})\}_2]_2$ (**2**), which was isolated as a yellow solid in 80% yield (Scheme 1). The ^1H and $^{13}C\{^1H\}$ NMR spectra of the solid, in dichloromethane-d_2, at room temperature (Figure S1 and S2) display resonances due to only one class of orthometalated phenylpyridine. Because the rupture of the chloride bridges, in dichloromethane, at room temperature is unlikely, this points out a symmetrical dimeric structure. In principle, both a racemic pair and a meso form are possible[14] (Figure S17). DFT calculations (B3LYP-D3//SDD(f)/6-31G**) reveal that the less sterically congested racemic mixture is 6.7 kcal·mol^{-1} more stable than the meso form.

Scheme 1. Bromination of the Dimer 1 with NBS

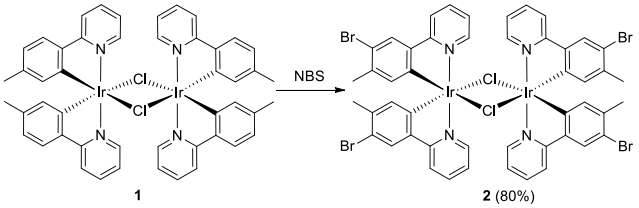

A noticeable feature of the bromination reaction of **2** to be highlighted is its high selectivity, including the absence of Br/Cl exchange, which is not consistent with a radical substitution reaction. We note that Leung and co-workers have carried out the treatment of the dimer $[Ir(\mu\text{-Cl})\{\kappa^2\text{-}C,N\text{-}(C_6H_4\text{-py})\}_2]_2$ with pyridinium tribromide in the presence of iron powder. In contrast to us, they isolated mixtures of $[Ir(\mu\text{-Br})\{\kappa^2\text{-}C,N\text{-}(C_6H_3Br\text{-py})\}_2]_2$ and $IrBr\{\kappa^2\text{-}C,N\text{-}(C_6H_3Br\text{-py})\}_2(py)$.[10c] The high selectivity observed in the reaction of Scheme 1 points toward a HOMO controlled nucleophilic substitution, as suggested by Aoki and co-workers.[9] In order to confirm it, we analyzed the HOMO distribution in **1** and in the successive brominated intermediates which should lead to **2** (Scheme 2).

Scheme 2. Intermediates for the Bromination of 1 to Give 2 Showing the HOMO Percentages on the Carbon Atoms of the Phenyl Groups

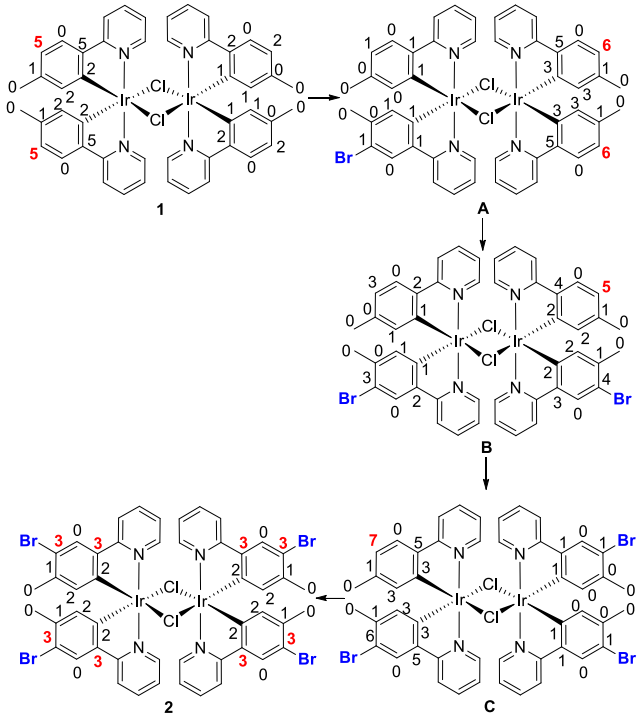

The HOMO of **1** spreads through the metal centers (45%) and the four orthometalated phenyl groups (48%), with higher contribution of two of them coordinated to the same iridium atom (16, 16, 7, and 7%). The analysis of the distribution within these rings reveals that the carbon atoms disposed in *para*-position with regard to the Ir−C bonds have the highest HOMO percentage (5% each one). The bromination of one of these centers affords the monobrominated intermediate **A**. The HOMO of the latter is mainly delocalized on the iridium atoms (45%) and the phenyl rings of the non-brominated mononuclear fragment (19 and 18%). The carbon atoms disposed *trans* to the Ir−C bonds are the centers of these rings displaying the highest HOMO percentage again. The bromination of one of them gives the dibrominated intermediate **B**. A similar analysis on **B** reveals that the following functionalized C−H bond should be that, *trans* disposed to the Ir−C bond, of one of the non-brominated phenyl groups. Its functionalization would give **C**, which could subsequently afford **2**. In summary, according to this analysis, the tetrabromination of **1** is a sequential process, which takes

https://doi.org/10.1021/acs.organomet.1c00408
Organometallics 2021, 40, 3211−3222

Scheme 3. Complex 2 as Starting Material for the Preparation of [3b + 3b + 3b′] Compounds

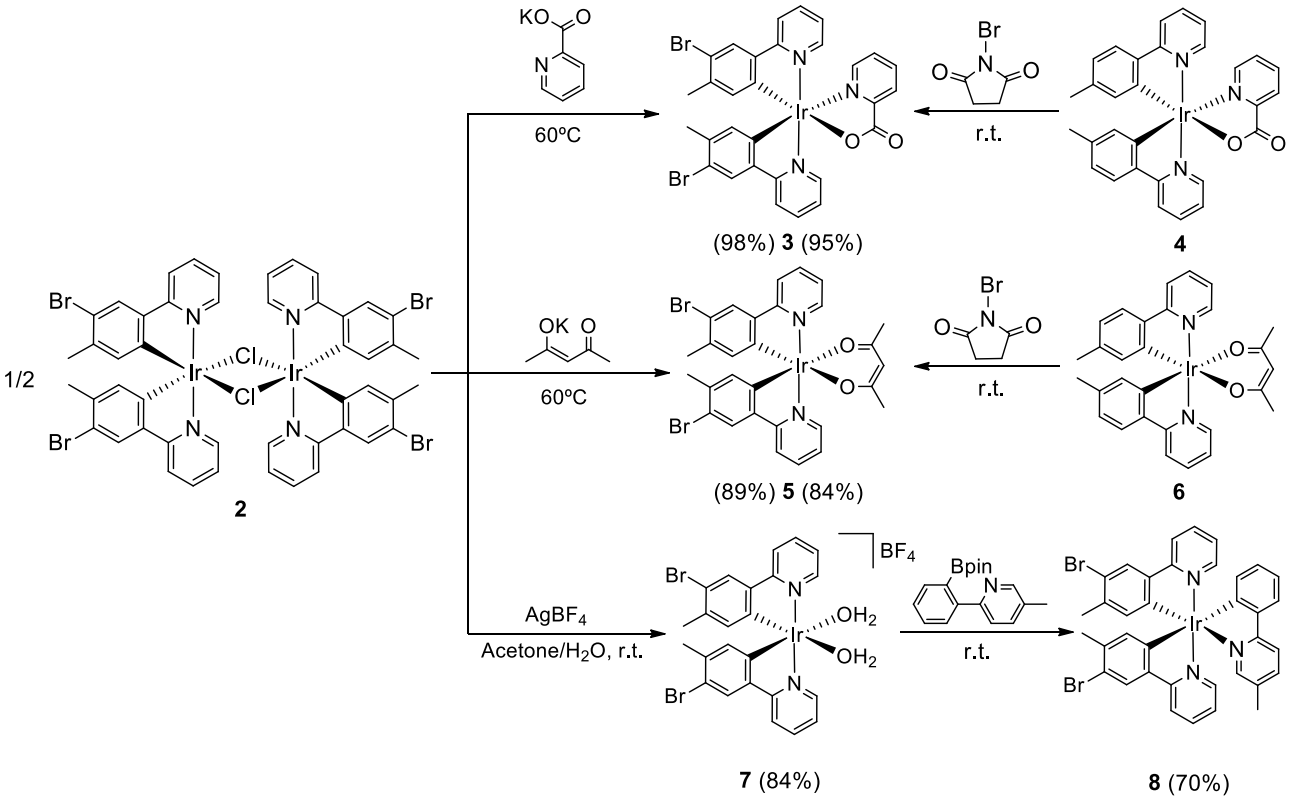

place in both mononuclear metal fragments in an alternate manner.

Dimer **2** is certainly an excellent starting compound to prepare brominated [3b + 3b + 3b′] emitters. As a proof of concept validation, three different compounds were synthesized in high yields starting from it (Scheme 3).

Treatment of tetrahydrofuran suspension of **2** with 2.1 equiv of 2-picolinic acid and 2.1 equiv of KOH, at 60 °C, for 1.5 h quantitatively leads to Ir{κ^2-*C,N*-(C_6H_2MeBr-py)}$_2${κ^2-*O,N*-[OC(O)-py]} (**3**), which can be also obtained in about 95% yield by bromination of Ir{κ^2-*C,N*-(C_6H_3Me-py)}$_2${κ^2-*O,N*-[OC(O)-py]} (**4**) with NBS in dichloromethane. In principle, one would expect that the asymmetry of the picolinate anion could generate some preference in the order of bromination of the phenyl rings of **4**. However, the analysis of the HOMO within these rings reveals that both have the same HOMO distribution (Chart 1).

Complex **3** was isolated as a yellow solid and characterized by X-ray diffraction analysis. Figure 1 shows a view of the molecule. The geometry around the iridium atom is the expected octahedron with the pyridyl groups of the orthometalated ligands situated mutually *trans* (N(1)−Ir−N(2) = 176.16(18)°). The picolinate anion lies at the perpendicular plane along with the metalated carbon atoms of the brominated groups (O(1)−Ir−C(1) = 173.37(16)° and N(3)−Ir−C(13) = 171.56(18)°). The asymmetry of the picolinate anion has a strong influence in the iridium-phenyl bonds, which is revealed by the Ir−C(1) and Ir−C(13) bond lengths. Thus, the former (1.979(5) Å) is about 0.05 Å shorter than the second one (2.026(5) Å), indicating a marked difference in *trans*-influence between the pyridyl ring and the CO_2 substituent. The structure shown in Figure 1 is consistent with the ^{1}H and ^{13}C{^{1}H} NMR spectra of the obtained solids,

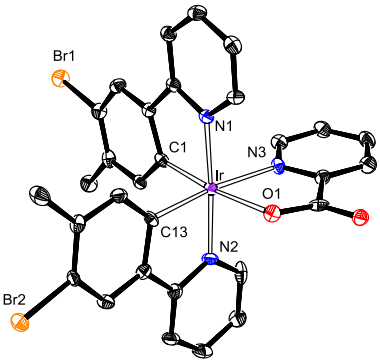

Figure 1. ORTEP diagram of complex **3** (50% probability ellipsoids). Hydrogen atoms are omitted for clarity. Selected bond lengths (Å) and angles (deg): Ir−N(1) = 2.034(4), Ir−N(2) = 2.046(4), Ir−N(3) = 2.136(4), Ir−O(1) = 2.162(4), Ir−C(1) = 1.979(5), Ir−C(13) = 2.026(5), N(1)−Ir−N(2) = 176.16(18), O(1)−Ir−C(1) = 173.37(16), N(3)−Ir−C(13) = 171.56(18).

Chart 1. HOMO Percentages on the Carbon Atoms of the Phenyl Groups of 4

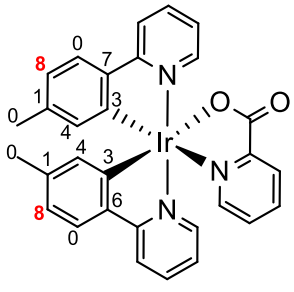

https://doi.org/10.1021/acs.organomet.1c00408
Organometallics 2021, 40, 3211−3222

in dichloromethane-d_2, at room temperature (Figure S3 and S4), the most noticeable feature of which being the presence of two singlets at 2.17 and 2.12 ppm in the ^{1}H spectrum, due to the methyl substituents of the inequivalent brominated phenyl groups.

The chloride bridge ligands of **2** can be also replaced by acetylacetonate (acac). The addition of 2.1 equiv of acetylacetone and 2.1 equiv of KOH to tetrahydrofuran suspensions of the dimer at 60 °C affords Ir{κ^2-*C*,*N*-(C_6H_2BrMe-py)}$_2${κ^2-*O*,*O*-(acac)} (**5**) in almost quantitative yield after 1.5 h. Similarly to **3**, the yellow complex **5** was further prepared by bromination of the acac-precursor Ir{κ^2-*C*,*N*-(C_6H_3Me-py)}$_2${κ^2-*O*,*O*-(acac)} (**6**), in 84% yield, and characterized by X-ray diffraction analysis. The structure (Figure 2) resembles that of **3** with the acac group in the

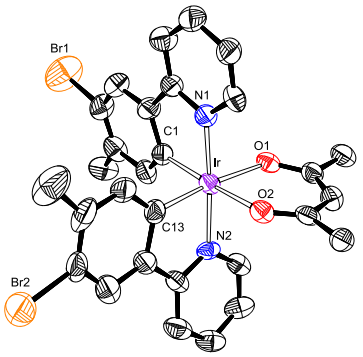

Figure 2. ORTEP diagram of complex **5** (50% probability ellipsoids). Hydrogen atoms are omitted for clarity. Selected bond lengths (Å) and angles (deg): Ir−N(1) = 2.034(10), Ir−N(2) = 2.044(10), Ir−O(1) = 2.133(8), Ir−O(2) = 2.135(8), Ir−C(1) = 1.994(12), Ir−C(13) = 1.979(13), N(1)−Ir−N(2) = 175.7(4), O(1)−Ir−C(13) = 173.8(4), O(2)−Ir−C(1) = 174.6(4).

position of the picolinate anion and N(1)−Ir−N(2), O(1)−Ir−C(13), and O(2)−Ir−C(1) angles of 175.7(4)°, 173.8(4), and 174.6(4)°, respectively. In contrast to **3**, the symmetry of the acac ligand gives rise to iridium−phenyl bonds statistically identical of 1.979(13) Å (Ir−C(13)) and 1.994(12) Å (Ir−C(1)). The presence of the acac group in the complex is also strongly supported by its ^{1}H and ^{13}C{^{1}H} NMR spectra, in dichloromethane-d_2, at room temperature (Figure S5 and S6), which contain the characteristic singlets of this ligand at 5.27 and 1.78 (^{1}H) and 185.2, 108.8, and 28.7 (^{13}C{^{1}H}) ppm.

The sequential addition of 2.0 mol of $AgBF_4$ and water to the acetone solutions of **2** quantitatively generates the solvento complex [Ir{κ^2-*C*,*N*-(C_6H_2BrMe-py)}$_2$(H_2O)$_2$]BF_4 (**7**), which was isolated as a yellow solid in 84% yield. The presence of the water ligands in this species was inferred from its ^{1}H NMR spectrum, in dichloromethane-d_2, at room temperature, which contains a broad resonance centered at 4.3 ppm (Figure S7). *cis*-Bis(aquo)iridium(III) compounds have proved to be aryl recipients from boronated aryl-proligands, in base-assisted transmetalation reactions.[15] In agreement with this, the treatment of the 2-propanol solutions of **7** with 1.5 equiv of 2-(2-pinacolborylphenyl)-5-methylpyridine in the presence of 40 equiv of K_3PO_4, at room temperature, for 24 h gives Ir{κ^2-*C*,*N*-(C_6H_2BrMe-py)}$_2${κ^2-*C*,*N*-[C_6H_4-Mepy]} (**8**), containing an orthometalated 2-phenyl-5-methylpyridine ligand instead of the picolinate or acac anions. Complex **8** was isolated as a yellow solid in 70% yield (59% with regard to **2**), after silica column chromatography purification, and characterized by X-ray diffraction analysis. The structure (Figure 3) proves the formation of the tris-pyridyl derivative and reveals a *mer*-

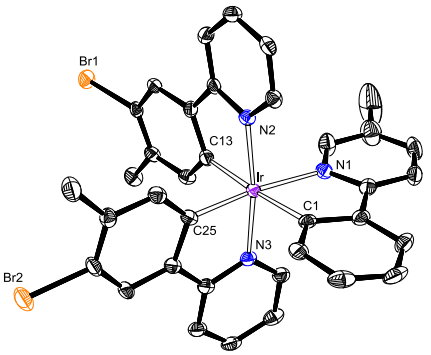

Figure 3. ORTEP diagram of complex **8** (50% probability ellipsoids). Hydrogen atoms are omitted for clarity. Selected bond lengths (Å) and angles (deg): Ir−N(1) = 2.131(4), Ir−N(2) = 2.049(3), Ir−N(3) = 2.038(3), Ir−C(1) = 2.077(4), Ir−C(13) = 2.081(4), Ir−C(25) = 1.999(4), N(2)−Ir−N(3) = 171.24(14), N(1)−Ir−C(25) = 172.64(15), C(1)−Ir−C(13) = 176.02(16).

disposition for the pyridyl rings. Thus, the coordination polyhedron around the metal center can be described as a distorted octahedron with the pyridyl groups of the brominated ligands mutually *trans* disposed (N(2)−Ir−N(3) = 171.24(14)°), whereas the pyridyl disubstituted ring and the metalated carbon atoms of the phenyl groups lie at the perpendicular plane, completing the metal coordination (N(1)−Ir−C(25) = 172.64(15)° and C(1)−Ir−C(13) = 176.02(16)°). The iridium-phenyl bond lengths of 2.077(4) (Ir−C(1)), 2.081(4) (Ir−C(13)), and 1.999(4) (Ir−C(25)) Å compare well with those of **3** and **5**. The structure is in accordance with ^{1}H and ^{13}C{^{1}H} NMR spectra of the compound, in dichloromethane-d_2, at room temperature (Figure S9 and S10). The most noticeable feature is the presence of three methyl resonances in each one of them, which appear at 2.20, 2.17, and 2.12 ppm in the ^{1}H spectrum and at 23.3, 23.2, and 18.3 ppm in the ^{13}C{^{1}H} one.

Cross-Coupling Reactions. These reactions are one of the most efficient tools to modify and enlarge the application range of phosphorescent emitters.[9c,13c,16] Thus, they have been employed to convert iridium(III) complexes bearing cyclometalated 2-phenylpyridines or related ligands into emissive polymers[17] and dendrimers.[18] Freixa and co-workers have appended azobenzene moieties to the phenyl group, to study the influence of the extended conjugation and substitution on the photochromic properties of the resulting systems.[19] Williams' group has assembled multimetallic broad-band light emitters, through coupling of mononuclear bis-terpyridyl complexes with extended conjugation.[20]

The C−C cross-coupling has been usually performed at no hindered positions. Although bromine sites in **5** and **8** are sterically hindered by the presence of the methyl group in *ortho*-position, these compounds undergo postfunctionalization by Suzuki−Miyaura cross-coupling, with R−B(OH)$_2$ (R = Me, Ph), according to Scheme 4. The reactions were carried out, in the presence of 4.0 equiv of K^{t}BuO, in 4:1 toluene:tetrahydrofuran mixtures as solvent, at 90 °C, using a 20% mol of (2-dicyclohexylphosphino,2′,6′-dimethoxybiphenyl)[2-(2′-amino-1,1-biphenyl]palladium(II)-methanesulfonate (Sphos-Pd) as catalyst precursor. Complex Sphos-Pd is a member of the palladium precatalysts family

https://doi.org/10.1021/acs.organomet.1c00408
Organometallics 2021, 40, 3211−3222

Scheme 4. Cross-Coupling Reactions for 5 and 8

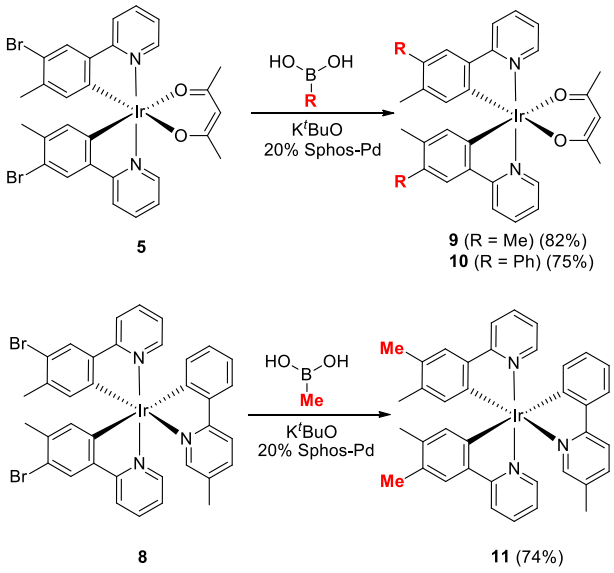

based on a 2-aminobiphenyl mesylate palladacycle, which easily generates the palladium(0) active species under the catalysis.[21] Under the reaction conditions, derivatives Ir{κ^2-*C,N*-(C_6H_2RMe-py)}$_2${κ^2-*O,O*-(acac)} (R = Me (**9**), Ph (**10**)) and Ir{κ^2-*C,N*-($C_6H_2Me_2$-py)}$_2${κ^2-*C,N*-[C_6H_4-Mepy]} (**11**) were quantitatively formed after 24 h and subsequently purified by silica column chromatography, to be isolated as yellow solids in 82, 75, and 74% yield, respectively.

Complex **11** was characterized by X-ray diffraction analysis. The structure (Figure 4) confirms the postfunctionalization of

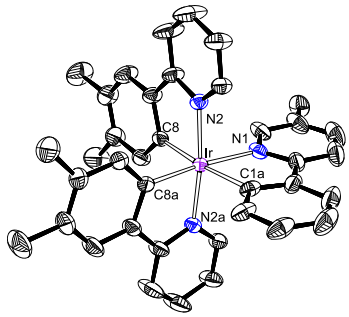

Figure 4. ORTEP diagram of complex **11** (50% probability ellipsoids). Hydrogen atoms are omitted for clarity. Selected bond lengths (Å) and angles (deg): Ir−N(1) = 2.117(3), Ir−N(2) = 2.034(3), Ir−N(2a) = 2.034(3), Ir−C(8) = 2.037(3), Ir−C(8a) = 2.037(3), N(2a)−Ir−N(2) = 172.42(14), N(1)−Ir−C(8a) = 173.36(12), C(1a)−Ir−C(8) = 173.36(12)°.

the brominated compounds. The coordination polyhedron around the metal center resembles that of **8**, with N(2a)−Ir−N(2), N(1)−Ir−C(8a), and C(1a)−Ir−C(8) angles of 172.42(14)°, 173.36(12)°, and 173.36(12)°, respectively.

Photophysical and Electrochemical Properties of the New [3b + 3b + 3b′] Emitters. Figures S18−S23 gather the UV−vis spectra of 10^{-5} M solutions of complexes **3**, **5**, and **8**−**11** in 2-methyltetrahydrofuran (2-MeTHF), at room temperature, whereas Tables 1 and S1−S12 summarize the main absorptions. In order to assign them we executed time-dependent DFT calculations (B3LYP-D3//SDD(f)/6-31G**) with tetrahydrofuran as solvent. Figures S25−S30 depict the frontier molecular orbitals. The spectra display three different zones: <300, 300−450, and >450 nm. The strong absorptions at the highest energy region are due to $^1\pi-\pi^*$ intra- and interligand transitions. Bands in the middle region, 300 and 450 nm, correspond to metal to ligand along with intraligand and ligand to ligand spin allowed charge transfers. The very weak absorption tails after 450 nm were assigned to formally spin forbidden transitions, mainly HOMO-to-LUMO, caused by the large spin−orbit coupling introduced by the 5d metal. The HOMO is delocalized between iridium atom (39−50%) and the 3b ligands (52−56%), whereas the LUMO spreads on the 3b ligands (89−96%) for **5** and **8**−**10** and on the 3b ligands (77 and 63%) and the 3b′ group (20 and 36%, respectively) for **3** and **11**.

The redox properties of the new emitters were evaluated by cyclic voltammetry, to gain more insight into their frontier orbitals. The experiments were performed under argon atmosphere, in dichloromethane solutions, with Bu_4NPF_6 as supporting electrolyte (0.1 M). Figure S24 provides the voltammograms, whereas Table 2 compiles the potentials versus Fc/Fc$^+$. The table furthermore collects the HOMO energy levels, calculated from the oxidation potentials, and the LUMO energy levels, estimated from the optical gap obtained from the onset of emission, as well as DFT-calculated values. Complexes **3**, **5**, **9**, and **10** exhibit a quasireversible Ir(III)/Ir(IV) oxidation, between 0.23 and 0.60 V, while complexes **8** and **11** display quasireversible oxidations from Ir(III)-to-Ir(IV) and from Ir(IV)-to-Ir(V) at 0.21 and 0.76 V and 0.00 and 0.58 V, respectively. Reduction peaks were not observed in the range from −1.5 to 1.5 V. The DFT-calculated HOMO−LUMO gap values are between 3.51 and 3.64 eV and depend upon the 3b′ ligand, decreasing as the picolinate anion is changed by an acac group and the latter by an orthometalated 2-phenyl-5-methylpyridine ligand. In addition, it diminishes when the bromides of the 3b ligands are replaced by methyl or phenyl; i.e., according to the sequence **3** > **5** > **8** = **10** ≥ **9** > **11**.

Complexes **3**, **5**, and **8**−**11** are green-yellow emitters (488−580 nm) upon photoexcitation in doped poly(methyl methacrylate) (PMMA) film at 5 wt %, at room temperature, and 2-MeTHF at room temperature and at 77 K (Figures S31−S48). Table 3 summarizes their main photophysical features, including experimental and calculated wavelengths, observed lifetimes, quantum yields, and radiative and non-radiative rate constants.

The experimental wavelengths agree well with those obtained through the estimation of the difference in energy between the optimized triplet states T_1 and the singlet states S_0 in tetrahydrofuran. This indicates that the emissions should be assigned to T_1 excited states. The emission wavelengths depend upon the chemical nature of the 3b′ ligand. The energy increases in the sequence **8** < **5** < **3**, observing a shift of the emission maximum toward blue as the orthometalated 2-phenyl-5-methylpyridine ligand is replaced by an acac group and the latter by the picolinate anion (Figure 5a), in good agreement with the increase of the HOMO−LUMO gap according to the same sequence. An evident fact resulting from the comparison of the spectra of Figure 5a is that picolinate and acac groups give rise to narrower emissions than the orthometalated 2-phenyl-5-methylpyridine ligand. This, which is highly desirable for the OLED application, seems to be related to a less pronounced difference between the excited-state structure and the ground-state structure for **3** and **5** than

https://doi.org/10.1021/acs.organomet.1c00408
Organometallics 2021, 40, 3211−3222

Table 1. Selected Calculated (TD-DFT in THF) and Experimental UV−Vis Absorptions for 3, 5, 8−11 (in 2-MeTHF) and Their Major Contributions

λ_{exp} (nm)	ε (M^{-1} cm^{-1})	exc. energy (nm)	oscillator strength, f	transition	character of the transition[a]
Complex **3**					
270	95 800	272	0.103	H-6 → L + 2 (54%)	(3b′ → 3b)
328	23 200	327	0.044	H-3 → L + 2 (58%)	(Ir + 3b → 3b)
360	10 800	359	0.0106	HOMO → L + 3 (95%)	(Ir + 3b → 3b + 3b′)
408	6900	425 (S_1)	0.0578	HOMO → LUMO (85%)	(Ir + 3b → 3b + 3b′)
457	3900	472 (T_1)	0	HOMO → LUMO (65%)	(Ir + 3b → 3b + 3b′)
Complex **5**					
273	89 374	268	0.4658	H-2 → L + 4 (42%)	(3b → 3b)
373	4014	376	0.0453	H-1 → L + 1 (95%)	(Ir + 3b′ → 3b)
420	2302	433 (S_1)	0.0547	HOMO → LUMO (97%)	(Ir + 3b → 3b)
470	1564	478 (T_1)	0	HOMO → LUMO (81%)	(Ir + 3b → 3b)
Complex **8**					
276	85 800	276	0.0532	H-6 → L + 2 (32%) H-4 → L + 3 (25%)	(3b′ → 3b)
390	12 300	378	0.0795	H-1 → L + 1 (79%)	(Ir + 3b′ → 3b + 3b′)
455	5200	434 (S_1)	0.0452	HOMO → LUMO (95%)	(Ir + 3b → 3b)
490	1900	472 (T_1)	0	HOMO → LUMO (66%)	(Ir + 3b → 3b)
Complex **9**					
281	41 500	260	0.0613	H-5 → L + 3 (40%)	(3b + 3b′ → 3b)
320	17 300	340	0.0988	H-3 → LUMO (86%)	(Ir + 3b → 3b)
375	5500	374	0.0412	H-1 → L + 1 (93%)	(Ir + 3b′ → 3b)
422	3100	441 (S_1)	0.0562	HOMO → LUMO (97%)	(Ir + 3b → 3b)
475	2500	490 (T_1)	0	HOMO → LUMO (82%)	(Ir + 3b → 3b)
Complex **10**					
278	103 500	270	0.0657	H-8 → L + 1 (47%)	(3b + 3b′ → 3b)
340	14200	339	0.101	H-3 → LUMO (89%)	(Ir + 3b → 3b)
379	7400	374	0.0436	H-1 → L + 1 (86%)	(Ir + 3b′ → 3b)
429	3700	437 (S_1)	0.0581	HOMO → LUMO (97%)	(Ir + 3b → 3b)
476	300	483 (T_1)	0	HOMO → LUMO (80%)	(Ir + 3b → 3b)
Complex **11**					
276	114 500	280	0.0725	H-7 → L + 1 (51%)	(3b → 3b + 3b′)
345	21 700	350	0.0435	H-2 → LUMO (70%)	(Ir + 3b + 3b′ → 3b + 3b′)
391	12300	383	0.0385	H-1→L+1 (93%)	(Ir + 3b + 3b′ → 3b + 3b′)
436	7100	442 (S_1)	0.439	HOMO → LUMO (85%)	(Ir + 3b → 3b + 3b′)
477	4500	482 (T_1)	0	HOMO → LUMO (56%)	(Ir + 3b → 3b + 3b′)

[a]3b = {κ^2-*C*,*N*-(C_6H_2BrMe-py)}, {κ^2-*C*,*N*-(C_6H_2RMe-py)}; 3b′ = {κ^2-*O*,*N*-[OC(O)-py]}, {κ^2-*O*,*O*-(acac)}, {κ^2-*C*,*N*-[C_6H_4-Mepy]}.

Table 2. Electrochemical and DFT Molecular Orbitals Energy Data for 3, 5, 8−11

		obs (eV)			calcd (eV)		
complex	$E^{1/2}_{ox}$ (V)	HOMO[a]	E_{00}[b]	LUMO[c]	HOMO[d]	LUMO[d]	HLG[d,e]
3	0.60	−5.40	2.60	−2.80	−5.16	−1.52	3.64
5	0.43	−5.23	2.55	−2.68	−5.04	−1.42	3.62
8	0.21, 0.76	−5.01	2.62	−2.39	−4.95	−1.37	3.58
9	0.23	−5.03	2.52	−2.51	−4.80	−1.23	3.57
10	0.32	−5.12	2.57	−2.55	−4.89	−1.31	3.58
11	0.00, 0.58	−4.80	2.61	−2.18	−4.71	−1.20	3.51

[a]HOMO = −[E_{ox} vs Fc/Fc^+ + 4.8] eV. [b]E_{00} = onset of emission in 2-MeTHF at 77 K. [c]LUMO = HOMO + E_{00}. [d]Values from DFT calculations. [e]HLG = LUMO − HOMO.

for **8**.[22] As expected from the reduction of the HOMO−LUMO gap as consequence of the replacement of the bromide substituent of the phenyl groups of the 3b ligands by phenyl and methyl, the performed cross-coupling reactions give rise to a slight red shift of the emission maximum of the resulting emitters, being bigger for methyl than for phenyl (Figure 5b). This is consistent with previous observations pointing out that the presence of halide substituents at the orthometalated phenyl group causes an increase in the energy of the emission.[13f,23] The number of replaced bromides also appears to influence the shift magnitude. In contrast to **5**, **9**, and **10**, the effect of the substitution on the emission of the monobrominated complex Ir{κ^2-*C*,*N*-(C_6H_3Br-py)}{κ^2-*C*,*N*-(C_6H_4-py)}{κ^2-*O*,*O*-(acac)} is negligible.[16c] This compound was prepared by activation of *ortho*-CH and *ortho*-CBr bonds of two different molecules of 2-(2-bromophenyl)pyridine on the same molecule of the dimer [Ir(μ-Cl)(COE)$_2$]$_2$ (COE = cyclooctene).[24] The emission spectra in PMMA film and in 2-

https://doi.org/10.1021/acs.organomet.1c00408
Organometallics 2021, 40, 3211−3222

Table 3. Photophysical Data of Complexes 3, 5, 8−11

calcd. λ_{em} (nm)[a]	medium (T, K)	λ_{em} (nm)	τ (μs)	ϕ	k_r (s^{-1})[b]	k_{nr} (s^{-1})[b]	k_r/k_{nr}
Complex **3**							
511	PMMA (298)	507	1.5	0.79	5.3×10^5	1.4×10^5	3.8
	2-MeTHF (298)	508	2.1	0.84	4.0×10^5	7.6×10^4	5.3
	2-MeTHF (77)	489, 526	3.7				
Complex **5**							
522	PMMA (298)	520	1.3	0.49	3.8×10^5	3.9×10^5	0.97
	2-MeTHF (298)	520	1.4	0.45	3.2×10^5	3.9×10^5	0.82
	2-MeTHF (77)	504, 541	3.0				
Complex **8**							
528	PMMA (298)	551	1.0	0.40	4.0×10^5	6.0×10^5	0.67
	2-MeTHF (298)	565	1.3	0.41	3.2×10^5	4.5×10^5	0.71
	2-MeTHF (77)	501, 531	3.7				
Complex **9**							
536	PMMA (298)	532	1.1	0.60	5.5×10^5	3.6×10^5	1.5
	2-MeTHF (298)	531	2.0	0.58	2.9×10^5	2.1×10^5	1.4
	2-MeTHF (77)	515, 552	4.8				
Complex **10**							
526	PMMA (298)	525	1.3	0.55	4.2×10^5	3.5×10^5	1.2
	2-MeTHF (298)	525	1.6	0.59	3.7×10^5	2.6×10^5	1.4
	2-MeTHF (77)	493, 532	5.0				
Complex **11**							
556	PMMA (298)	580	1.2	0.47	3.9×10^5	4.4×10^5	0.89
	2-MeTHF (298)	577	1.6	0.50	3.1×10^5	3.1×10^5	1.0
	2-MeTHF (77)	488, 526	5.0				

[a]From the DFT optimized structures (THF, 298 K, ZPE(T_1)-ZPE(S_0)). [b]$k_r = \varphi/\tau$ and $k_{nr} = (1-\varphi)/\tau$, being k_r the radiative rate constant, k_{nr} the nonradiative rate constant, φ the quantum yield, and τ the lifetime of the triplet excited-state.

MeTHF at room temperature display broad structureless bands. However, they have vibronic fine structures in 2-MeTHF at 77 K. Figure 5c shows the spectra of complex **3**. This suggests a significant contribution of ligand-centered $^3\pi-\pi^*$ transitions to the excited state.[25]

The lifetimes are short and lie in a narrow range of 1.0−5.0 μs. The quantum yields, as the maximum of the emissions, depend upon the nature of 3b′ ligand and the substituents of the orthometalated phenyl group of the 3b ligands. The quantum yields of the picolinate derivative **3** in PMMA and in 2-MeTHF at room temperature are about 0.80. The replacement of the picolinate anion by an acac group decreases the quantum yield values until close 0.50 and the replacement of the latter by an orthometalated 2-phenyl-5-methylpyridine ligand to 0.40. The substitution of the bromide at the 3b ligands of the acac derivative **5** by methyl or phenyl, to afford **9** or **10**, gives rise to an increase of the quantum yields, which reach about 0.60. Similarly, the change of bromide by methyl in **8** to form **11** improves the quantum yield to 0.50. Although the effect of the substitution of bromide by methyl and phenyl on the quantum yield is in this case moderate, it lies in line with that observed for the replacement of the bromide of the monobrominated compound Ir{κ^2-*C*,*N*-(C_6H_3Br-py)}{κ^2-*C*,*N*-(C_6H_4-py)}{κ^2-*O*,*O*-(acac)} by the same organic fragments.[16c] In contrast, the incorporation of phenyl or methyl to the orthometalated phenyl groups of Ir{κ^2-*C*,*N*-[C_6H_4-py]}$_3$ produces a significant decrease in the emission quantum yield.[26] The radiative and nonradiative rate constants have values of the same magnitude order and the ratio between them is close to the unit.

CONCLUDING REMARKS

This study shows the selective bromination, with *N*-bromosuccinimide, of the C−H bonds disposed in *para*-position, with regard to the Ir−C bonds, of the phenyl substituent of the orthometalated 2-phenylpyridine ligands of a [Ir(μ-Cl)(3b)$_2$]$_2$ dimer. The tetrabromination is HOMO directed and occurs in sequential and alternate manner in both mononuclear metal fragments. The resulting functionalized dimer is the origin of several types of functionalized iridium(III) phosphorescent green-yellow emitters of class [3b + 3b + 3b′], which are easily and cleanly obtained in high yield, by replacement of the chloride bridges by 3b′ ligands. These functionalized emitters allow a subsequent postfunctionalization through C−C cross-coupling reactions catalyzed by a palladium-phosphine complex. Their photophysical properties are dependent on the 3b′ ligands and, once it has been established the 3b′ ligand, they can be fine-tuned by means of the replacement of the bromine atoms by alkyl or aryl groups, via cross-coupling reactions.

In summary, the selective bromination of the phenyl substituent of the orthometalated 2-phenyl-pyridine ligands of dimers [Ir(μ-Cl)(3b)$_2$]$_2$, with *N*-bromosuccinimide, is a nice synthetic methodology of C−H functionalization, to implement the preparation of iridium(III) phosphorescent emitters, which allows subsequent postfunctionalization and prevents issues of unwanted reactions in successive steps.

EXPERIMENTAL SECTION

General Information. All reactions were carried out with exclusion of air using Schlenk-tube techniques or in a drybox. Instrumental methods are given in the Supporting Information. Chemical shifts (expressed in ppm) are referenced to residual solvent peaks. Signals were assigned using also bidimensional NMR

https://doi.org/10.1021/acs.organomet.1c00408
Organometallics 2021, 40, 3211−3222

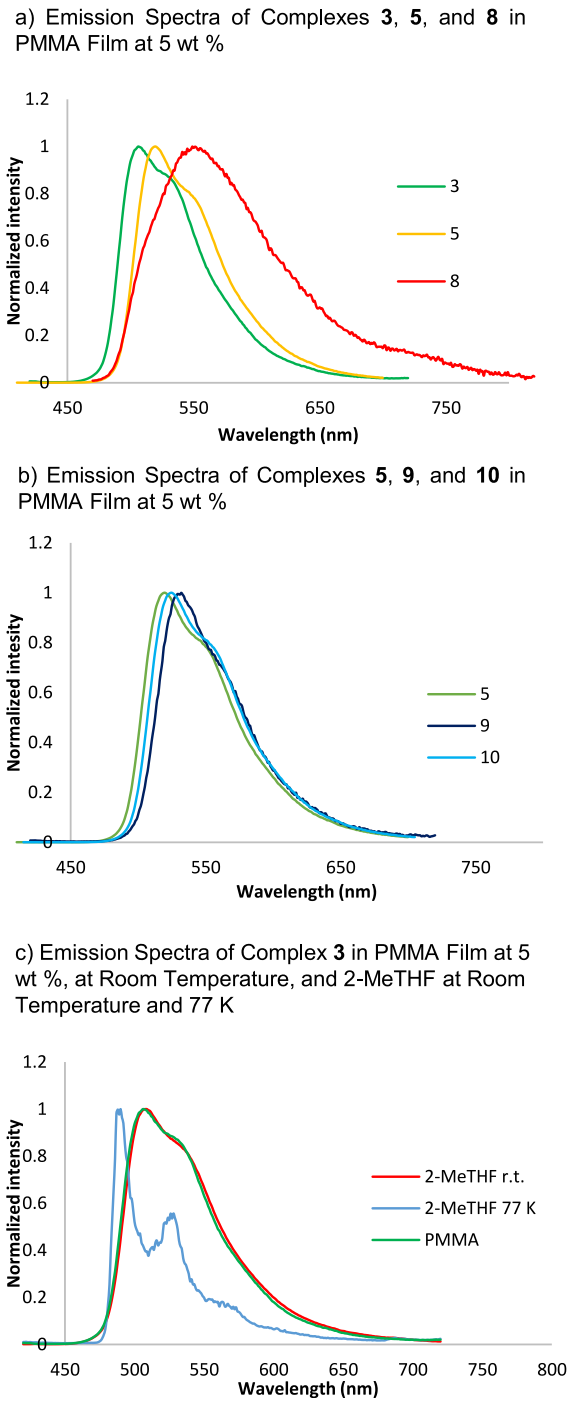

Figure 5. Emission spectra for complexes **3**, **5**, and **8**−**10**.

experiments (^{1}H−^{1}H COSY, ^{1}H−^{13}C{^{1}H} HMBC and ^{1}H−^{13}C{^{1}H} HSQC). The complexes [Ir(μ-Cl){κ^2-*C,N*-(C_6H_3Me-py)}]$_2$ (**1**), Ir{κ^2-*C,N*-(C_6H_3Me-py)}$_2${κ^2-*O,N*-[OC(O)-py]} (**4**), and Ir{κ^2-*C,N*-(C_6H_3Me-py)}$_2${κ^2-*O,O*-(acac)} (**6**) were prepared as published.[27]

Reaction of [Ir(μ-Cl){κ^2-*C,N*-(C_6H_3Me-py)}]$_2$ (1) with *N*-Bromosuccinimide: Preparation of [Ir(μ-Cl){κ^2-*C,N*-(C_6H_2MeBr-py)}]$_2$ (2). *N*-Bromosuccinimide (315.6 mg, 1.77 mmol) was added to a solution of [Ir(μ-Cl){κ^2-*C,N*-(C_6H_3Me-py)}]$_2$ (**1**) (500 mg, 0.443 mmol) in 15 mL of dichloromethane. The reaction was stirred for 24 h at room temperature. After that time, the green suspension was filtered over Celite to obtain a green solution which was concentrated almost to dryness under a vacuum. The addition of 5 mL of diethyl ether afforded a yellow solid which was decanted and washed with more diethyl ether (3 × 5 mL) and dried under a vacuum. Yield: 512 mg (80%). Elemental analysis calcd. for $C_{48}H_{36}Br_4Ir_2N_4$: C: 39.93; H: 2.51; N: 3.88, found C: 40.12; H: 2.46; N: 3.75. HRMS (electrospray) *m/z* calcd for $C_{24}H_{18}Br_2IrN_2$ [M-Ir(Br-*p*-tolylpyridine)$_2$Cl$_2$]$^+$: 686.9432, found 686.9485. ^{1}H NMR (Figure S1) (300 MHz, CD_2Cl_2, 298 K) δ 9.14 (4H, CH py), 7.85 (8H, CH py), 7.70 (4H, CH Ph), 6.83 (4H, CH py), 5.69 (4H, CH Ph), 2.00 (12H, CH_3). ^{13}C{^{1}H}-apt NMR (Figure S2) (75 MHz, CD_2Cl_2, 298 K) δ 167.0 (4C, C py), 151.8 (4C, CH py), 144.4 (4C, C−Ir), 143.3 (4C, C Ph), 139.0 (4C, C−Br), 137.4 (4C, CH py), 132.9 (4C, CH Ph), 127.5 (4C, CH Ph), 123.3 (4C, CH py), 119.3 (4C, CH py), 118.3 (4C, C-Me), 23.2 (4C, CH_3).

Preparation of Ir{κ^2-*C,N*-(C_6H_2MeBr-py)}$_2${κ^2-*O,N*-[OC(O)-py]} (3). This complex was prepared by two different procedures:

(a) Picolinic acid (45.9 mg, 0.372 mmol) and KOH (24.6 mg, 0.373 mmol) in 2 mL of methanol were added to a suspension of **2** (200 mg, 0.139 mmol) in 15 mL of THF. The mixture was stirred at 60 °C for 90 min. After that time, the suspension was dried under a vacuum, treated with 15 mL of dichloromethane, and filtered over Celite. The resulting yellow solution was concentrated under a vacuum almost to dryness. The addition of 5 mL of pentane gave rise a yellow solid which was washed with more pentane (2 × 4 mL) and finally was dried under a vacuum. Yield: 220 mg (98%).

(b) *N*-Bromosuccinimide (274.1 mg, 1.54 mmol) was added to a solution of **4** (500 mg, 0.768 mmol) in 15 mL of dichloromethane. The reaction was stirred for 2 h. After that time the green suspension was filtered over Celite to obtain a dark green solution. This solution was concentrated almost to dryness. The addition of diethyl ether afforded a yellow solid, which was washed with 3 × 5 mL of diethyl ether and dried under a vacuum. Yield: 590 mg (95%). X-ray quality crystals were grown by slow diffusion of pentane into a concentrated solution of the solid in dichloromethane at 4 °C. Elemental analysis calcd. for $C_{30}H_{22}Br_2IrN_3O_2$: C: 44.56; H: 2.74; N: 5.20, found C: 44.36; H: 2.57; N: 5.12. IR (cm^{-1}) ν(C═O) = 1650 (s). HRMS (electrospray) *m/z* calcd for $C_{30}H_{22}Br_2IrN_3NaO_2$ [M + Na]$^+$: 831.9573, found 831.9537. ^{1}H NMR (Figure S3) (300 MHz, CD_2Cl_2, 298 K) δ 8.66 (1H, CH py), 8.23 (1H, CH py or Ph), 7.83 (8H, CH py or Ph), 7.46 (1H, CH py or Ph), 7.36 (1H, CH py or Ph), 7.17 (1H, CH py), 6.99 (1H, CH py or Ph), 6.23 (s, 1H, CH Ph), 6.03 (s, 1H, CH Ph), 2.17 (3H, CH_3), 2.12 (3H, CH_3). ^{13}C{^{1}H}-apt NMR (Figure S4) (75 MHz, CD_2Cl_2, 298 K) δ 167.6, 166.5 (2C, C Ph), 152.5 (C py or Ph), 149.1 (CH py), 148.9, 148.7 (2C, CH py or Ph), 148.2, 146.2, 144.9, 144.8, 139.8, 139.3 (6C, C py or Ph), 138.4, 138.1, 138.0 (3C, CH py or Ph), 135.1, 135.0 (2C, CH Ph), 128.5, 128.3, 128.0, 123.1, 123.0, 119.7 119.2 (7C, CH py or Ph), 118.5, 118.0 (2C, C py or Ph), 23.2 (2C, CH_3).

Preparation of Ir{κ^2-*C,N*-(C_6H_2BrMe-py)}$_2${κ^2-*O,O*-(acac)} (5). This complex was prepared by two different procedures:

(a) Acetylacetone (82 μL, 0.812 mmol) and KOH (53.6 mg, 0.812 mmol) in 2 mL of methanol were added to a suspension of **2** (550 mg, 0.381 mmol) in 15 mL of THF. The mixture was stirred at 60 °C for 90 min. After that time, the suspension was dried under a vacuum. The residue was treated with 15 mL of dichloromethane and the resulting suspension was filtered over Celite. The yellow solution was concentrated under a vacuum almost to dryness. The addition of 5 mL of pentane led to a yellow solid which was washed with more pentane (2 × 4 mL) and dried under a vacuum. Yield: 533 mg (89%).

(b) *N*-Bromosuccinimide (113.4 mg, 0.637 mmol) was added to a solution of **6** (200 mg, 0.318 mmol) in 10 mL of dichloromethane. The mixture was stirred for 24 h at room temperature. After that time, the green suspension was filtered over Celite to obtain a green solution which was concentrated almost to dryness under a vacuum. The addition of 5 mL of diethyl ether gave rise to a yellow solid which was decanted and washed with more diethyl ether (3 × 5 mL) and dried under a vacuum. Yield: 174 mg (84%). X-ray quality crystals were grown by slow diffusion of pentane into a concentrated solution of the solid in dichloromethane at 4 °C. Elemental analysis calcd. for $C_{29}H_{25}Br_2IrN_2O_2$: C: 44.34; H: 3.21; N: 3.57, found C: 44.63; H: 3.15; N: 3.32. IR (cm^{-1}) ν(C═O) = 1579 (s). HRMS (electrospray) *m/z* calcd for $C_{24}H_{18}Br_2IrN_2$ [M − acac]$^+$: 686.9432, found 686.9477. ^{1}H NMR (Figure S5) (300 MHz, CD_2Cl_2, 298 K) δ 8.43 (2H, CH

https://doi.org/10.1021/acs.organomet.1c00408
Organometallics 2021, 40, 3211−3222

py), 7.81 (4H, CH py), 7.72 (2H, CH Ph), 7.20 (2H, CH py), 6.08 (2H, CH Ph), 5.27 (1H, acac-H), 2.10 (6H, Ph−CH_3), 1.78 (6H, acac-CH_3). $^{13}C\{^1H\}$-apt NMR (Figure S6) (75 MHz, CD_2Cl_2, 298 K) δ 185.2 (2C, C═O acac), 167.1 (2C, C py), 148.6 (2C, C−H py), 146.1 (2C, C Ph), 145.7 (2C, C−Ir), 138.5 (2C, C−Br), 137.8 (2C, C−H py), 135.8, 127.6 (4C, C−H Ph), 122.5, 119.0 (4C, C−H py), 117.7 (2C, *C*-CH_3), 100.8 (CH acac), 28.7 (2C, CH_3 acac), 23.1 (2C, CH_3).

Preparation of [Ir{κ^2-*C*,*N*-(C_6H_2BrMe-py)}$_2$(H_2O)$_2$]BF_4 (7). Silver tetrafluoroborate (134.9 mg, 0.693 mmol) was added to a solution of **2** (500 mg, 0.346 mmol) in 15 mL of acetone. The suspension was stirred for 2 h in absence of light and filtered over Celite to afford a yellow solution. Then, water (500 μL, 27.7 mmol) was added and the solution was stirred for 1 h. After that time, the resulting solution was dried under a vacuum and pentane (2 × 5 mL) was added to break the oily product. Yield 468 mg (84%). Elemental analysis calcd. for $C_{24}H_{22}BBr_2F_4IrN_2O_2$: C: 35.62, H: 2.74, N: 3.46, found C: 35.79, H: 3.11, N: 3.26. IR (cm^{-1}) ν(H_2O) 3434, (br), ν(BF_4) 1042 (s). HRMS (electrospray) *m*/*z* calcd for $C_{24}H_{18}Br_2IrN_2$ [M − $2H_2O$]$^+$: 686.9432, found 686.9458. ^1H NMR (Figure S7) (300 MHz, CD_2Cl_2, 298 K) δ 8.90 (2H, CH py), 7.93 (2H, CH py), 7.86 (2H, CH py), 7.71 (2H, CH Ph), 7.42 (2H, CH py), 5.96 (2H, CH Ph), 4.57−4.02 (4H, broad, H_2O), 2.09 (6H, CH_3). $^{13}C\{^1H\}$-apt NMR (Figure S8) (75 MHz, CD_2Cl_2, 298 K) δ 166.1 (4C, C py and Ph), 150.0 (2C, CH py), 145.4 (2C, C−Ir), 139.6 (2C, *C*-CH_3), 139.5 (2C, CH py), 135.6 (2C, CH Ph), 134.0 (2C, C−Br), 128.0 (2C, CH Ph), 123.7 (2C, CH py). 119.5 (2C, CH py), 23.2 (2C, CH_3).

Preparation of Ir{κ^2-*C*,*N*-(C_6H_2BrMe-py)}$_2${κ^2-*C*,*N*-[C_6H_4-Mepy]} (8). 2-(2-Pinacolborylphenyl)-5-methylpyridine (256 mg, 0.867 mmol) and K_3PO_4 (4.91 g, 23.12 mmol) were added to a solution of **7** (468 mg, 0.578 mmol) in 30 mL of 2-propanol. The resulting orange suspension was stirred for 24 h. After that time, the suspension was dried under a vacuum. The residue was treated with 30 mL of dichloromethane and filtered over Celite. The solution was concentrated almost to dryness. The addition of pentane (2 × 5 mL) gave a yellow solid which was purified by a silica column chromatography using toluene as eluent. Yield 342 mg (70%). X-ray quality crystals were grown by slow diffusion of pentane into a concentrated solution of the solid in dichloromethane at 4 °C. Elemental analysis calcd. for $C_{36}H_{28}Br_2IrN_3$: C: 50.59; H: 3.30; N: 4.92, found C: 50.35; H: 3.33; N: 4.84. HRMS (electrospray) *m*/*z* calcd for $C_{24}H_{18}Br_2IrN_2$ [M − MePyPh]$^+$: 686.9432, found 686.945. ^1H NMR (Figure S9) (300 MHz, CD_2Cl_2, 298 K) δ 8.04 (1H, CH py), 7.86 (2H, CH py or Ph), 7.76 (5H, CH py or Ph), 7.55 (4H, CH py or Ph), 6.95 (1H, CH py or Ph), 6.89 (1H, CH py or Ph), 6.78 (3H, CH py or Ph), 6.43 (1H, CH Ph), 6.24 (1H, CH Ph), 2.20, 2.17, 2.12 (9H, 3 CH_3). $^{13}C\{^1H\}$-apt NMR (Figure S10) (75 MHz, CD_2Cl_2, 298 K) δ 175.6 (C py or Ph), 174.1 (C Ph), 169.3 (C py or Ph), 166.6 (C py or Ph), 166.0 (C py or Ph), 158.5 (C py or Ph), 153.5 (CH py), 151.4 (CH py or Ph), 148.4 (CH py or Ph), 146.0 (C−Ir), 145.6 (C−Ir), 143.3 (C−Ir), 139.2 (C py or Ph), 138.9 (C py or Ph), 138.2 (CH py or Ph), 137.8 (CH py or Ph), 136.3 (CH py or Ph), 135.7 (CH Ph), 135.0 (CH py or Ph), 133.3 (CH Ph), 132.9 (C py or Ph), 129.9, 128.1, 127.7, 124.4, 122.8, 122.1, 121.9, 119.2, 118.9 (9C, CH py or Ph), 118.0 (*C*-CH_3), 115.6 (*C*-CH_3), 23.3, 23.2, 18.3 (3C, CH_3).

Preparation of Ir{κ^2-*C*,*N*-($C_6H_2Me_2$-py)}$_2${κ^2-*O*,*O*-(acac)} (9). A Schlenk with a PTFE stopcock was charged with **5** (250 mg, 0.318 mmol), methylboronic acid (114.2 mg, 1.91 mmol), potassium *tert*-butoxide (142.8 mg, 1.27 mmol), Sphos-Pd (49.6 mg, 0.0636 mmol), 8 mL of toluene and 2 mL of THF. The yellow solution was stirred in the dark, at 90 °C for 24 h. After that time, the mixture was dried under a vacuum. The crude was purified by silica column chromatography, using toluene as eluent, to afford a yellow solid. Yield: 172 mg (82%). Elemental analysis calcd. for $C_{31}H_{31}IrN_2O_2$: C: 56.78; H: 4.76; N: 4.27, found C: 57.03; H: 4.45; N: 3.98. IR (cm^{-1}) ν(C═O) = 1579 (s). HRMS (electrospray) *m*/*z* calcd for $C_{31}H_{31}IrN_2O_2$ [M$^+$]: 656.2011, found 656.2069. ^1H NMR (Figure S11) (300 MHz, CD_2Cl_2, 298 K) δ 8.45 (2H, CH py), 7.85−7.79 (2H, CH py), 7.77−7.70 (2H, CH py), 7.35 (2H, CH Ph), 7.12 (2H, CH py), 5.97 (2H, CH Ph), 5.25 (1H, CH acac), 2.14 (6H, Ph−CH_3), 1.98 (6H, Ph−CH_3), 1.77 (6H, CH_3 acac). $^{13}C\{^1H\}$-apt NMR (Figure S12) (75 MHz, CD_2Cl_2, 298 K) δ 184.9 (2C, C═O acac), 168.9 (2C, C py), 148.5 (2C, CH py), 144.1 (2C, C Ph), 143.3 (2C, C−Ir), 138.3 (2C, C Ph), 137.2 (2C, CH py), 134.7 (2C, CH Ph), 129.1 (2C, C Ph), 125.3 (2C, CH Ph), 121.4 (2C, CH py), 118.4 (2C, CH py), 100.6 (CH acac), 28.8 (2C, CH_3 acac), 20.0 (2C, Ph-CH_3), 19.5 (2C, CH_3).

Preparation of Ir{κ^2-*C*,*N*-(C_6H_2PhMe-py)}$_2${κ^2-*O*,*O*-(acac)} (10). A Schlenk with a PTFE stopcock was charged with **5** (200 mg, 0.255 mmol), phenylboronic acid (124.4 mg, 1.02 mmol), potassium *tert*-butoxide (114.5 mg, 1.02 mmol), Sphos-Pd (39.7 mg, 0.0509 mmol), 8 mL of toluene and 2 mL of THF. The yellow solution was stirred in the dark, at 90 °C for 24 h. After that time, the mixture was dried under a vacuum. The crude was purified by silica column chromatography, using toluene as eluent, to afford a yellow solid. Yield: 150 mg (75%). Elemental analysis calcd. for $C_{31}H_{31}IrN_2O_2$: C: 56.78; H: 4.76; N: 4.27, found C: 56.52; H: 4.87; N: 4.12. IR (cm^{-1}) ν(C═O) = 1577(s). HRMS (electrospray) *m*/*z* calcd for $C_{36}H_{28}IrN_2$ [M − acac]$^+$: 681.1878, found 681.1864. ^1H NMR (Figure S13) (300 MHz, CD_2Cl_2, 298 K) δ 8.51 (2H, CH py), 7.88−7.80 (2H, CH py or Ph), 7.81−7.70 (2H, CH py or Ph), 7.45 (2H, CH Ph), 7.42−7.25 (10H, CH py or Ph), 7.23−7.14 (2H, CH py or Ph), 6.17 (2H, CH Ph), 5.29 (1H, CH acac), 2.01 (6H, CH_3 Ph), 1.82 (6H, CH_3 acac). $^{13}C\{^1H\}$-apt NMR (Figure S14) (75 MHz, CD_2Cl_2, 298 K) δ 185.1 (2C, C═O acac), 168.6 (2C, C py), 148.6 (2C, CH py), 146.5 (2C, C Ph), 143.8 (2C, C Ph), 143.0 (2C, C Ph), 137.5 (2C, CH py or Ph), 136.8 (2C, C py or Ph), 135.4 (2C, CH py or Ph), 129.8 (4C, CH Ph), 128.4 (4C, CH Ph), 126.7 (2C, CH py or Ph), 125.5 (2C, CH py or Ph), 122.0 (2C, CH py or Ph), 118.8 (2C, CH py or Ph), 100.8 (CH acac), 28.8 (2C, CH_3 acac), 20.8 (2C, Ph-CH_3).

Preparation of Ir{κ^2-*C*,*N*-($C_6H_2Me_2$-py)}$_2${κ^2-*C*,*N*-[C_6H_4-Mepy]} (11). A Schlenk with a PTFE stopcock was charged with **8** (150 mg, 0.176 mmol), methylboronic acid (63.0 mg, 1.05 mmol), potassium *tert*-butoxide (79 mg, 0.704 mmol), Sphos-Pd (27.2 mg, 0.0352 mmol), 8 mL of toluene and 2 mL of THF. The yellow solution was stirred in the dark, at 90 °C for 24 h. After that time, the mixture was dried under a vacuum. The crude was purified by column chromatography, using toluene as eluent, to obtain a yellow solid. Yield: 95 mg (74%). X-ray quality crystals were grown by slow evaporation of the solvent of a concentrated solution of the solid in pentane at 4 °C. Elemental analysis calcd. for $C_{38}H_{34}IrN_3$: C: 62.96; H: 4.73; N: 5.80, found C: 63.12; H: 4.95; N: 5.63. HRMS (electrospray) *m*/*z* calcd for $C_{26}H_{24}IrN_2$ [M − MePyPh]$^+$: 557.1594, found 557.1576. ^1H NMR (Figure S15) (300 MHz, CD_2Cl_2, 298 K) δ 8.06 (1H, CH py), 7.91−7.71 (6H, CH py or Ph), 7.65−7.44 (6H, CH py or Ph), 7.00−6.91 (1H, CH py or Ph), 6.92−6.86 (2H, CH py or Ph), 6.76−6.70 (1H, CH py or Ph), 6.36 (1H, CH Ph), 6.17 (1H, CH Ph), 2.23, 2.21, 2.14, 2.10, 2.09 (15H, 5 CH_3). $^{13}C\{^1H\}$-apt NMR (Figure S16) (75 MHz, CD_2Cl_2, 298 K) δ 177.7 (C py or Ph), 172.5 (C py or Ph), 171.3 (C Ph), 171.3, 168.3, 166.3, 156.9 (4C, C py or Ph), 153.4 (CH py), 151.6 (CH py or Ph), 148.3 (CH py or Ph), 146.2, 143.2, 140.7 (3C, C−Ir), 139.1, 138.9 (2C, C py or Ph), 138.1, 137.8, 135.7, 134.4, (4C, CH py or Ph), 134.3 (CH Ph), 132.5 (C py or Ph), 132.1 (CH Ph), 129.6 (CH py or Ph), 128.9, 126.9 (2C, C py or Ph), 125.7, 125.3, 124.3, 121.7, 121.5, 121.0, 119.0, 118.7, 118.4 (9C, CH py or Ph), 20.3, 20.2, 19.9, 19.7, 18.3 (5C, CH_3).

■ ASSOCIATED CONTENT

Supporting Information

The Supporting Information is available free of charge at https://pubs.acs.org/doi/10.1021/acs.organomet.1c00408.

General information for the experimental section; crystallographic data; computational details; cyclic voltammograms; experimental and computed UV−vis spectra; frontier molecular orbitals and natural transition

https://doi.org/10.1021/acs.organomet.1c00408
Organometallics 2021, 40, 3211−3222

orbitals; normalized excitation and emission spectra; and NMR spectra (PDF)

Cartesian coordinates of the optimized structures (XYZ)

Accession Codes

CCDC 2091180−2091183 contain the supplementary crystallographic data for this paper. These data can be obtained free of charge via www.ccdc.cam.ac.uk/data_request/cif, or by emailing data_request@ccdc.cam.ac.uk, or by contacting The Cambridge Crystallographic Data Centre, 12 Union Road, Cambridge CB2 1EZ, UK; fax: +44 1223 336033.

AUTHOR INFORMATION

Corresponding Author

Miguel A. Esteruelas − *Departamento de Química Inorgánica, Instituto de Síntesis Química y Catálisis Homogénea (ISQCH), Centro de Innovación en Química Avanzada (ORFEO−CINQA), Universidad de Zaragoza−CSIC, 50009 Zaragoza, Spain;* orcid.org/0000-0002-4829-7590; Email: maester@unizar.es

Authors

Pierre-Luc T. Boudreault − *Universal Display Corporation, Ewing, New Jersey 08618, United States*

Erik Mora − *Departamento de Química Inorgánica, Instituto de Síntesis Química y Catálisis Homogénea (ISQCH), Centro de Innovación en Química Avanzada (ORFEO−CINQA), Universidad de Zaragoza−CSIC, 50009 Zaragoza, Spain*

Enrique Oñate − *Departamento de Química Inorgánica, Instituto de Síntesis Química y Catálisis Homogénea (ISQCH), Centro de Innovación en Química Avanzada (ORFEO−CINQA), Universidad de Zaragoza−CSIC, 50009 Zaragoza, Spain;* orcid.org/0000-0003-2094-719X

Jui-Yi Tsai − *Universal Display Corporation, Ewing, New Jersey 08618, United States;* orcid.org/0000-0002-8516-9985

Complete contact information is available at: https://pubs.acs.org/10.1021/acs.organomet.1c00408

Notes

The authors declare no competing financial interest.

ACKNOWLEDGMENTS

Financial support from the MINECO of Spain (PID2020-115286GB-I00 and RED2018-102387-T (AEI/FEDER, UE), Gobierno de Aragón (E06_20R and LMP148_18), FEDER, and the European Social Fund is acknowledged

REFERENCES

(1) (a) Davies, H. M. L.; Morton, D. Recent Advances in C-H Functionalization. *J. Org. Chem.* **2016**, *81*, 343−350. (b) Hartwig, J. F.; Larsen, M. A. Undirected, Homogeneous C-H Bond Functionalization: Challenges and Opportunities. *ACS Cent. Sci.* **2016**, *2*, 281−292. (c) Dixneuf, P. H.; Doucet, H. C-H Bond Activation and Catalytic Functionalization I. *Top. Organomet. Chem.* **2016**, *55*, 217−258. (d) Dalton, T.; Faber, T.; Glorius, F. C-H Activation: Toward Sustainability and Applications. *ACS Cent. Sci.* **2021**, *7*, 245−261.

(2) (a) Corbet, J.-P.; Mignani, G. Selected Patented Cross-Coupling Reaction Technologies. *Chem. Rev.* **2006**, *106*, 2651−2710. (b) Johansson Seechurn, C. C. C.; Kitching, M. O.; Colacot, T. J.; Snieckus, V. Palladium-Catalyzed Cross-Coupling: A Historical Contextual Perspective to the 2010 Nobel Prize. *Angew. Chem., Int. Ed.* **2012**, *51*, 5062−5085. (c) Campeau, L.-C.; Hazari, N. Cross-Coupling and Related Reactions: Connecting Past Success to the Development of New Reactions for the Future. *Organometallics* **2019**, *38*, 3−35. (d) Kadu, B. S. Suzuki-Miyaura Cross Coupling Reaction: Recent Advancements in Catalysis and Organic Synthesis. *Catal. Sci. Technol.* **2021**, *11*, 1186−1221.

(3) (a) Petrone, D. A.; Ye, J.; Lautens, M. Modern Transition-Metal-Catalyzed Carbon-Halogen Bond Formation. *Chem. Rev.* **2016**, *116*, 8003−8104. (b) Lied, F.; Patra, T.; Glorius, F. Group 9 Transition Metal-Catalyzed C-H Halogenations. *Isr. J. Chem.* **2017**, *57*, 945−952. (c) Das, R.; Kapur, M. Transition-Metal-Catalyzed Site-Selective C-H Halogenation Reactions. *Asian J. Org. Chem.* **2018**, *7*, 1524−1541.

(4) Saikia, I.; Borah, A. J.; Phukan, P. Use of Bromine and Bromo-Organic Compounds in Organic Synthesis. *Chem. Rev.* **2016**, *116*, 6837−7042.

(5) See, for example: (a) Wang, B.-Y.; Karikachery, A. R.; Li, Y.; Singh, A.; Lee, H. B.; Sun, W.; Sharp, P. R. Remarkable Bromination and Blue Emission of 9-Anthracenyl Pt(II) Complexes. *J. Am. Chem. Soc.* **2009**, *131*, 3150−3151. (b) Karikachery, A. R.; Masjedi, M.; Sharp, P. R. Thermal and Photochemical Ring-Bromination in Naphthyl-, Naphthdiyl-, and Dicarboximideperyl-Platinum Complexes. *Organometallics* **2015**, *34*, 1635−1642.

(6) Koval, I. V. N-Halo Reagents. N-Halosuccinimides in Organic Synthesis and in Chemistry of Natural Compounds. *Russ. J. Org. Chem.* **2002**, *38*, 301−337.

(7) Warratz, S.; Burns, D. J.; Zhu, C.; Korvorapun, K.; Rogge, T.; Scholz, J.; Jooss, C.; Gelman, D.; Ackermann, L. *meta*-C-H Bromination on Purine Bases by Heterogeneous Ruthenium Catalysis. *Angew. Chem., Int. Ed.* **2017**, *56*, 1557−1560.

(8) Yu, Q.; Hu, L. A.; Wang, Y.; Zheng, S.; Huang, J. Directed *meta*-Selective Bromination of Arenes with Ruthenium Catalysts. *Angew. Chem., Int. Ed.* **2015**, *54*, 15284−15288.

(9) (a) Aoki, S.; Matsuo, Y.; Ogura, S.; Ohwada, H.; Hisamatsu, Y.; Moromizato, S.; Shiro, M.; Kitamura, M. Regioselective Aromatic Substitution Reactions of Cyclometalated Ir(III) Complexes: Synthesis and Photochemical Properties of Substituted Ir(III) Complexes That Exhibit Blue, Green, and Red Color Luminescence Emission. *Inorg. Chem.* **2011**, *50*, 806−818. (b) Tamura, Y.; Hisamatsu, Y.; Kumar, S.; Itoh, T.; Sato, K.; Kuroda, R.; Aoki, S. Efficient Synthesis of Tris-Heteroleptic Iridium(III) Complexes Based on the Zn^{2+}-Promoted Degradation of Tris-Cyclometalated Iridium(III) Complexes and Their Photophysical Properties. *Inorg. Chem.* **2017**, *56*, 812−833. (c) Hisamatsu, Y.; Kumar, S.; Aoki, S. Design and Synthesis of Tris-Heteroleptic Cyclometalated Iridium(III) Complexes Consisting of Three Different Nonsymmetric Ligands Based on Ligand-Selective Electrophilic Reactions Via Interligand Homo Hopping Phenomena. *Inorg. Chem.* **2017**, *56*, 886−899. (d) Tamura, Y.; Hisamatsu, Y.; Kazama, A.; Yoza, K.; Sato, K.; Kuroda, R.; Aoki, S. Stereospecific Synthesis of Tris-Heteroleptic Tris-Cyclometalated Iridium(III) Complexes Via Different Heteroleptic Halogen-Bridged Iridium(III) Dimers and Their Photophysical Properties. *Inorg. Chem.* **2018**, *57*, 4571−4589.

(10) (a) Clark, A. M.; Rickard, C. E. F.; Roper, W. R.; Wright, L. J. Electrophilic Substitution Reactions at the Phenyl Ring of the Chelated 2-(2′-Pyridyl)phenyl Ligand Bound to Ruthenium(II) or Osmium(II). *Organometallics* **1999**, *18*, 2813−2820. (b) Cheung, K.-M.; Zhang, Q.-F.; Chan, K.-W.; Lam, M. H. W.; Williams, I. D.; Leung, W.-H. Direct Functionalization of the Cyclometalated 2-(2′-Pyridyl)phenyl Ligand Bound to Iridium(III). *J. Organomet. Chem.* **2005**, *690*, 2913−2921. (c) Gagliardo, M.; Snelders, D. J. M.; Chase, P. A.; Klein Gebbink, R. J. M.; van Klink, G. P. M.; van Koten, G. Organic Transformations on σ-Aryl Organometallic Complexes. *Angew. Chem., Int. Ed.* **2007**, *46*, 8558−8573. (d) Clark, G. R.; Johns, P. M.; Roper, W. R.; Wright, L. J. A Stable Iridabenzene Formed from an Iridacyclopentadiene Where the Additional Ring-Carbon Atom Is Derived from a Thiocarbonyl Ligand. *Organometallics* **2008**, *27*, 451−454. (e) Clark, G. R.; Johns, P. M.; Roper, W. R.; Söhnel, T.; Wright, L. J. Regioselective Mono-, Di-, and Trifunctionalization of Iridabenzofurans through Electrophilic Substitution Reactions. *Organometallics* **2011**, *30*, 129−138.

(11) See, for example: (a) You, Y.; Nam, W. Photofunctional Triplet Excited States of Cyclometalated Ir(III) Complexes: Beyond Electroluminescence. *Chem. Soc. Rev.* **2012**, *41*, 7061−7084. (b) Zanoni, K. P. S.; Coppo, R. L.; Amaral, R. C.; Murakami Iha, N. Y. Ir(III) Complexes Designed for Light-Emitting Devices: Beyond the Luminescence Color Array. *Dalton Trans.* **2015**, *44*, 14559−14573. (c) Omae, I. Application of the Five-Membered Ring Blue Light-Emitting Iridium Products of Cyclometalation Reactions as OLEDs. *Coord. Chem. Rev.* **2016**, *310*, 154−169. (d) Henwood, A. F.; Zysman-Colman, E. Lessons Learned in Tuning the Optoelectronic Properties of Phosphorescent Iridium(III) Complexes. *Chem. Commun.* **2017**, *53*, 807−826. (e) Li, T.-Y.; Wu, J.; Wu, Z.-G.; Zheng, Y.-X.; Zuo, J.-L.; Pan, Y. Rational Design of Phosphorescent Iridium(III) Complexes for Emission Color Tunability and Their Applications in OLEDs. *Coord. Chem. Rev.* **2018**, *374*, 55−92. (f) Lee, S.; Han, W.-S. Cyclometalated Ir(III) Complexes Towards Blue-Emissive Dopant for Organic Light-Emitting Diodes: Fundamentals of Photophysics and Designing Strategies. *Inorg. Chem. Front.* **2020**, *7*, 2396−2422.

(12) (a) Lalevée, J.; Peter, M.; Dumur, F.; Gigmes, D.; Blanchard, N.; Tehfe, M.-A.; Morlet-Savary, F.; Fouassier, J. P. Subtle Ligand Effects in Oxidative Photocatalysis with Iridium Complexes: Application to Photopolymerization. *Chem. - Eur. J.* **2011**, *17*, 15027−15031. (b) Prier, C. K.; Rankic, D. A.; MacMillan, D. W. C. Visible Light Photoredox Catalysis with Transition Metal Complexes: Applications in Organic Synthesis. *Chem. Rev.* **2013**, *113*, 5322−5363. (c) Arias-Rotondo, D. M.; McCusker, J. K. The Photophysics of Photoredox Catalysis: A Roadmap for Catalyst Design. *Chem. Soc. Rev.* **2016**, *45*, 5803−5820. (d) Tehfe, M.-A.; Lepeltier, M.; Dumur, F.; Gigmes, D.; Fouassier, J.-P.; Lalevée, J. Structural Effects in the Iridium Complex Series: Photoredox Catalysis and Photoinitiation of Polymerization Reactions under Visible Lights. *Macromol. Chem. Phys.* **2017**, *218*, 1700192. (e) Marzo, L.; Pagire, S. K.; Reiser, O.; König, B. Visible-Light Photocatalysis: Does It Make a Difference in Organic Synthesis? *Angew. Chem., Int. Ed.* **2018**, *57*, 10034−10072.

(13) See, for example: (a) Duan, Y.-C.; Wu, Y.; Ren, X.-Y.; Zhao, L.; Geng, Y.; Zhang, M.; Sun, G.-Y.; Su, Z.-M. From Blue to Full Color - Theoretical Design and Characterization of a Series of Ir(III) Complexes Containing Azoline Ligand with Potential Application in OLEDs. *Dalton Trans.* **2017**, *46*, 11491−11502. (b) Benjamin, H.; Liang, J.; Liu, Y.; Geng, Y.; Liu, X.; Zhu, D.; Batsanov, A. S.; Bryce, M. R. Color Tuning of Efficient Electroluminescence in the Blue and Green Regions Using Heteroleptic Iridium Complexes with 2-Phenoxyoxazole Ancillary Ligands. *Organometallics* **2017**, *36*, 1810−1821. (c) Davidson, R.; Hsu, Y.-T.; Bhagani, C.; Yufit, D.; Beeby, A. Exploring the Chemistry and Photophysics of Substituted Picolinates Positional Isomers in Iridium(III) Bisphenylpyridine Complexes. *Organometallics* **2017**, *36*, 2727−2735. (d) Sarma, M.; Tsai, W.-L.; Lee, W.-K.; Chi, Y.; Wu, C.-C.; Liu, S.-H.; Chou, P.-T.; Wong, K.-T. Anomalously Long-Lasting Blue Pholed Featuring Phenyl-Pyrimidine Cyclometalated Iridium Emitter. *Chem.* **2017**, *3*, 461−476. (e) Lai, P.-N.; Brysacz, C. H.; Alam, M. K.; Ayoub, N. A.; Gray, T. G.; Bao, J.; Teets, T. S. Highly Efficient Red-Emitting Bis-Cyclometalated Iridium Complexes. *J. Am. Chem. Soc.* **2018**, *140*, 10198−10207. (f) Benjamin, H.; Zheng, Y.; Kozhevnikov, V. N.; Siddle, J. S.; O'Driscoll, L. J.; Fox, M. A.; Batsanov, A. S.; Griffiths, G. C.; Dias, F. B.; Monkman, A. P.; Bryce, M. R. Unusual Dual-Emissive Heteroleptic Iridium Complexes Incorporating Tadf Cyclometalating Ligands. *Dalton Trans.* **2020**, *49*, 2190−2208.

(14) (a) Sprouse, S.; King, K. A.; Spellane, P. J.; Watts, R. J. Photophysical Effects of Metal-Carbon σ Bonds in Ortho-Metalated Complexes of Ir (III) and Rh (III). *J. Am. Chem. Soc.* **1984**, *106*, 6647−6653. (b) Garces, F. O.; Dedeian, K.; Keder, N. L.; Watts, R. J. Structures of *ortho*-Metalated [2-(*p*-Tolyl)Pyridine]Iridium(III) Complexes. *Acta Crystallogr., Sect. C: Cryst. Struct. Commun.* **1993**, *49*, 1117−1120. (c) McGee, K. A.; Mann, K. R. Selective Low-Temperature Syntheses of Facial and Meridional Tris-Cyclometalated Iridium(III) Complexes. *Inorg. Chem.* **2007**, *46*, 7800−7809. (d) Chien, C.-H.; Fujita, S.; Yamoto, S.; Hara, T.; Yamagata, T.; Watanabe, M.; Mashima, K. Stepwise and One-Pot Syntheses of Ir(III) Complexes with Imidazolium-Based Carbene Ligands. *Dalton Trans.* **2008**, 916−923. (e) Davies, D. L.; Lowe, M. P.; Ryder, K. S.; Singh, K.; Singh, S. Tuning Emission Wavelength and Redox Prperties Trough Potion of the Substituent in Iridium(III) Cyclometallated Complexes. *Dalton Trans.* **2011**, *40*, 1028−1030. (f) Congrave, D. G.; Hsu, Y.-T.; Batsanov, A. S.; Beeby, A.; Bryce, M. R. Synthesis, Diastereomer Separation, and Optoelectronic and Structural Properties of Dinuclear Cyclometalated Iridium(III) Complexes with Bridging Diarylhydrazide Ligands. *Organometallics* **2017**, *36*, 981−993. (g) Boudreault, P.-L. T.; Esteruelas, M. A.; López, A. M.; Oñate, E.; Raga, E.; Tsai, J.-Y. Insertion of Unsaturated C-C Bonds into the O-H Bond of an Iridium(III)-Hydroxo Complex: Formation of Phosphorescent Emitters with an Asymmetrical β-Diketonate Ligand. *Inorg. Chem.* **2020**, *59*, 15877−15887.

(15) (a) Maity, A.; Anderson, B. L.; Deligonul, N.; Gray, T. G. Room-Temperature Synthesis of Cyclometalated Iridium(III) Complexes: Kinetic Isomers and Reactive Functionalities. *Chem. Sci.* **2013**, *4*, 1175−1181. (b) Adamovich, V.; Bajo, S.; Boudreault, P.-L. T.; Esteruelas, M. A.; López, A. M.; Martín, J.; Oliván, M.; Oñate, E.; Palacios, A. U.; San-Torcuato, A.; Tsai, J.-Y.; Xia, C. Preparation of Tris-Heteroleptic Iridium(III) Complexes Containing a Cyclometalated Aryl-N-Heterocyclic Carbene Ligand. *Inorg. Chem.* **2018**, *57*, 10744−10760.

(16) (a) Kataoka, Y.; Okuno, K.; Yano, N.; Ueda, H.; Kawamoto, T.; Handa, M. New Luminescent Cyclometalated Iridium Complexes Prepared by the Post-Synthetic Modification. *J. Photochem. Photobiol., A* **2018**, *358*, 345−355. (b) Davidson, R. J.; Hsu, Y. T.; Yufit, D.; Beeby, A. Emission Tuning of Ir($\hat{\text{NC}}$)$_2$(Pic)-Based Complexes Via Torsional Twisting of Picolinate Substituents. *Organometallics* **2018**, *37*, 2003−2006. (c) Boudreault, P.-L. T.; Esteruelas, M. A.; Mora, E.; Oñate, E.; Tsai, J.-Y. Suzuki-Miyaura Cross-Coupling Reactions for Increasing the Efficiency of Tris-Heteroleptic Iridium(III) Emitters. *Organometallics* **2019**, *38*, 2883−2887.

(17) (a) Schulz, G. L.; Holdcroft, S. Conjugated Polymers Bearing Iridium Complexes for Triplet Photovoltaic Devices. *Chem. Mater.* **2008**, *20*, 5351−5355. (b) Yan, Q.; Yue, K.; Yu, C.; Zhao, D. Oligo- and Polyfluorene-Tethered *Fac*-Ir(Ppy)$_3$: Substitution Effects. *Macromolecules* **2010**, *43*, 8479−8487. (c) Guo, T.; Guan, R.; Zou, J.; Liu, J.; Ying, L.; Yang, W.; Wu, H.; Cao, Y. Red Light-Emitting Hyperbranched Fluorene-Alt-Carbazole Copolymers with an Iridium Complex as the Core. *Polym. Chem.* **2011**, *2*, 2193−2203. (d) Guo, T.; Yu, L.; Zhao, B.; Li, Y.; Tao, Y.; Yang, W.; Hou, Q.; Wu, H.; Cao, Y. Highly Efficient, Red-Emitting Hyperbranched Polymers Utilizing a Phenyl-Isoquinoline Iridium Complex as the Core. *Macromol. Chem. Phys.* **2012**, *213*, 820−828. (e) Hohenleutner, A.; Schmidbauer, S.; Vasold, R.; Joosten, D.; Stoessel, P.; Buchholz, H.; König, B. Rapid Combinatorial Synthesis and Chromatography Based Screening of Phosphorescent Iridium Complexes for Solution Processing. *Adv. Funct. Mater.* **2012**, *22*, 3406−3413. (f) Liang, A.-H.; Zhang, K.; Zhang, J.; Huang, F.; Zhu, X.-H.; Cao, Y. Supramolecular Phosphorescent Polymer Iridium Complexes for High-Efficiency Organic Light-Emitting Diodes. *Chem. Mater.* **2013**, *25*, 1013−1019. (g) Lian, M.; Yu, Y.; Zhao, J.; Huang, Z.; Yang, X.; Zhou, G.; Wu, Z.; Wang, D. Novel Phosphorescent Polymers Containing Both Ambipolar Segments and Functionalized Ir(III) Phosphorescent Moieties: Synthesis, Photophysical, Redox, and Electrophosphorescence Investigation. *J. Mater. Chem. C* **2014**, *2*, 9523−9535. (h) Guo, T.; Yu, L.; Yang, Y.; Li, Y.; Tao, Y.; Hou, Q.; Ying, L.; Yang, W.; Wu, H.; Cao, Y. Hyperbranched Red Light-Emitting Phosphorescent Polymers Based on Iridium Complex as the Core. *J. Lumin.* **2015**, *167*, 179−185.

(18) (a) Lai, W.-Y.; Levell, J. W.; Jackson, A. C.; Lo, S.-C.; Bernhardt, P. V.; Samuel, I. D. W.; Burn, P. L. A Phosphorescent Poly(Dendrimer) Containing Iridium(III) Complexes: Synthesis and Light-Emitting Properties. *Macromolecules* **2010**, *43*, 6986−6994. (b) Stoltzfus, D. M.; Jiang, W.; Brewer, A. M.; Burn, P. L. Twisted Dendrons for Highly Luminescent Green Emissive Phosphorescent Dendrimers. *J. Mater. Chem. C* **2018**, *6*, 10315−10326.

https://doi.org/10.1021/acs.organomet.1c00408
Organometallics 2021, 40, 3211−3222

(19) (a) Pérez-Miqueo, J.; Telleria, A.; Muñoz-Olasagasti, M.; Altube, A.; García-Lecina, E.; de Cózar, A.; Freixa, Z. Azobenzene-Functionalized Iridium(III) Triscyclometalated Complexes. *Dalton Trans.* **2015**, *44*, 2075−2091. (b) Pérez-Miqueo, J.; Altube, A.; García-Lecina, E.; Tron, A.; McClenaghan, N. D.; Freixa, Z. Photoswitchable Azobenzene-Appended Iridium(III) Complexes. *Dalton Trans.* **2016**, *45*, 13726−13741.
(20) (a) Leslie, W.; Batsanov, A. S.; Howard, J. A. K.; Williams, J. A. G. Cross-Couplings in the Elaboration of Luminescent Bis-Terpyridyl Iridium Complexes: The Effect of Extended or Inhibited Conjugation on Emission. *Dalton Trans.* **2004**, 623−631. (b) Whittle, V. L.; Williams, J. A. G. A New Class of Iridium Complexes Suitable for Stepwise Incorporation into Linear Assemblies: Synthesis, Electrochemistry, and Luminescence. *Inorg. Chem.* **2008**, *47*, 6596−6607. (c) Whittle, V. L.; Williams, J. A. G. Cyclometallated, Bis-Terdentate Iridium Complexes as Linearly Expandable Cores for the Construction of Multimetallic Assemblies. *Dalton Trans.* **2009**, 3929−3940. (d) Muñoz-Rodríguez, R.; Buñuel, E.; Fuentes, N.; Williams, J. A. G.; Cárdenas, D. J. A Heterotrimetallic Ir(III), Au(III) and Pt(II) Complex Incorporating Cyclometallating Bi- and Tridentate Ligands: Simultaneous Emission from Different Luminescent Metal Centres Leads to Broad-Band Light Emission. *Dalton Trans.* **2015**, *44*, 8394−8405. (e) Knuckey, K. J.; Williams, J. A. G. Photon Funnels for One-Way Energy Transfer: Multimetallic Assemblies Incorporating Cyclometallated Iridium or Rhodium Units Accessed by Sequential Cross-Coupling and Bromination. *Eur. J. Inorg. Chem.* **2017**, *2017*, 5205−5214.
(21) Bruno, N. C.; Tudge, M. T.; Buchwald, S. L. Design and Preparation of New Palladium Precatalysts for C-C and C-N Cross-Coupling Reactions. *Chem. Sci.* **2013**, *4*, 916−920.
(22) (a) Alabau, R. G.; Esteruelas, M. A.; Oliván, M.; Oñate, E.; Palacios, A. U.; Tsai, J.-Y.; Xia, C. Osmium(II) Complexes Containing a Dianionic CCCC-Donor Tetradentate Ligand. *Organometallics* **2016**, *35*, 3981−3995. (b) Alabau, R. G.; Esteruelas, M. A.; Oliván, M.; Oñate, E. Preparation of Phosphorescent Osmium(IV) Complexes with N,N′,C- and C,N,C′-Pincer Ligands. *Organometallics* **2017**, *36*, 1848−1859.
(23) (a) Tamayo, A. B.; Alleyne, B. D.; Djurovich, P. I.; Lamansky, S.; Tsyba, I.; Ho, N. N.; Bau, R.; Thompson, M. E. Synthesis and Characterization of Facial and Meridional Tris-Cyclometalated Iridium(III) Complexes. *J. Am. Chem. Soc.* **2003**, *125*, 7377−7387. (b) Li, J.; Djurovich, P. I.; Alleyne, B. D.; Yousufuddin, M.; Ho, N. N.; Thomas, J. C.; Peters, J. C.; Bau, R.; Thompson, M. E. Synthetic Control of Excited-State Properties in Cyclometalated Ir(III) Complexes Using Ancillary Ligands. *Inorg. Chem.* **2005**, *44*, 1713−1727. (c) Dedeian, K.; Shi, J.; Shepherd, N.; Forsythe, E.; Morton, D. C. Photophysical and Electrochemical Properties of Heteroleptic Tris-Cyclometalated Iridium(III) Complexes. *Inorg. Chem.* **2005**, *44*, 4445−4447. (d) Ragni, R.; Plummer, E. A.; Brunner, K.; Hofstraat, J. W.; Babudri, F.; Farinola, G. M.; Naso, F.; De Cola, L. Blue Emitting Iridium Complexes: Synthesis, Photophysics and Phosphorescent Devices. *J. Mater. Chem.* **2006**, *16*, 1161−1170. (e) Avilov, I.; Minoofar, P.; Cornil, J.; De Cola, L. Influence of Substituents on the Energy and Nature of the Lowest Excited States of Heteroleptic Phosphorescent Ir(III) Complexes: A Joint Theoretical and Experimental Study. *J. Am. Chem. Soc.* **2007**, *129*, 8247−8258. (f) Esteruelas, M. A.; López, A. M.; Oñate, E.; San-Torcuato, A.; Tsai, J.-Y.; Xia, C. Preparation of Phosphorescent Iridium(III) Complexes with a Dianionic C,C,C,C-Tetradentate Ligand. *Inorg. Chem.* **2018**, *57*, 3720−3730.
(24) Boudreault, P.-L. T.; Esteruelas, M. A.; Mora, E.; Oñate, E.; Tsai, J.-Y. Pyridyl-Directed C-H and C-Br Bond Activations Promoted by Dimer Iridium-Olefin Complexes. *Organometallics* **2018**, *37*, 3770−3779.
(25) (a) Hsieh, C.-H.; Wu, F.-I.; Fan, C.-H.; Huang, M.-J.; Lu, K.-Y.; Chou, P.-Y.; Yang, Y.-H. O.; Wu, S.-H.; Chen, I.-C.; Chou, S.-H.; Wong, K.-T.; Cheng, C.-H. Design and Synthesis of Iridium Bis(Carbene) Complexes for Efficient Blue Electrophosphorescence. *Chem. - Eur. J.* **2011**, *17*, 9180−9187. (b) Zanoni, K. P. S.; Kariyazaki, B. K.; Ito, A.; Brennaman, M. K.; Meyer, T. J.; Murakami Iha, N. Y. Blue-Green Iridium(III) Emitter and Comprehensive Photophysical Elucidation of Heteroleptic Cyclometalated Iridium(III) Complexes. *Inorg. Chem.* **2014**, *53*, 4089−4099.
(26) Kim, J.-H.; Kim, S.-Y.; Cho, D. W.; Son, H.-J.; Kang, S. O. Influence of Bulky Substituents on the Photophysical Properties of Homoleptic Iridium(III) Complexes. *Phys. Chem. Chem. Phys.* **2019**, *21*, 6908−6916.
(27) (a) Lamansky, S.; Djurovich, P.; Murphy, D.; Abdel-Razzaq, F.; Kwong, R.; Tsyba, I.; Bortz, M.; Mui, B.; Bau, R.; Thompson, M. E. Synthesis and Characterization of Phosphorescent Cyclometalated Iridium Complexes. *Inorg. Chem.* **2001**, *40*, 1704−1711. (b) Shin, I.-S.; Yoon, S.; Kim, J. I.; Lee, J.-K.; Kim, T. H.; Kim, H. Efficient Green-Colored Electrochemiluminescence from Cyclometalated Iridium(III) Complex. *Electrochim. Acta* **2011**, *56*, 6219−6223.

https://doi.org/10.1021/acs.organomet.1c00408
Organometallics 2021, 40, 3211−3222